1974

Kinetics of a Moving Boundary Ion-Exchange Process

Paul R. Dana
Iowa State University

Thomas D. Wheelock
Iowa State University, wheel@iastate.edu

Kinetics of a Moving Boundary Ion-Exchange Process

Abstract
The acid elution of the dark blue cupric ammine complex from a cation-exchange resin produced a sharply defined moving boundary within each bead, which was photographed and measured to provide rate data. 'Analysis of the data by means of a theoretical model indicated that the overall elution process was controlled by a combination of internal and external mass transfer when acid concentrations less than 1.0 N were employed. At these acid concent1'ations the interdiffusion coefficient for the resin phase was found to be 3 X 10-6 cm2/sec, independent of acid concentration but somewhat dependent on particle size. Data collected at· higher acid concentrations were not amenable to analysis by the method employed. The model should be useful for predicting the time required to elute the cupric ammine complex or for designing equipment to carry out this process.

Disciplines
Catalysis and Reaction Engineering | Complex Fluids | Other Chemical Engineering

pin-Tsai equations, the equations become the ordinary "rule of mixtures," that is

$$K = K_1\phi_1 + K_2\phi_2 \tag{6}$$

When $A \rightarrow 0$, the equations become the inverse rule of mixtures

$$\frac{1}{K} = \frac{\phi_1}{K_1} + \frac{\phi_2}{K_2} \tag{7}$$

Intermediate values of A give mixture rules which are between these upper and.lower bounds.

Acknowledgment

The work described in this paper is a part of the research conducted by the Monsanto/Washington University Association sponsored by the Advanced Research Projects Agency, Department of Defense, under Office of Naval Research Contract N00014-67-C-0218, formerly N00014-66-C-0045.

Literature Cited

Ashton, J. E., Halpin, J. C., Petit, P. H., "Primer on Composite Analysis," Chapter 5, p 72, Technomic, Stamford, Conn., 1969.
Behrens, E., *J. Compos. Mater.* **2**, 2 (1968).
Bruggeman, D. A. G., *Ann. Phys.* **24**, 636 (1935).
Burgers, J. M., "Second Report on Viscosity and Plasticity," p 113, Nordemann, New York, N. Y., 1938.
Cheng, S. C., Vachon, R. I., *Int. J. Heat Mass Transfer* **12**, 249 (1969).
Einstein, A., *Ann. Phys.* **17**, 549 (1905).
Einstein, A., *Ann. Phys.* **19**, 289 (1906).
Halpin, J. C., *J. Compos. Mater.* **3**, 732 (1969).
Hamilton, R. L., Crosser, O. K., *Ind. Eng. Chem., Fundam.* **1**, 187 (1962).
Hashin, Z., *Appl. Mech. Rev.* **17**, 1 (1964).
Hashin, Z., Rosen, B. W., *J. Appl. Mech.* **E31**, 223 (1964).
Hashin, Z. Shtrikman, S., *J. Mech. Phys. Solids* **11**, 127 (1963).
Hill, R., *J. Mech. Phys. Solids* **13**, 189 (1965).
Kerner, E. H., *Proc. Phys. Soc.* **B69**, 802, 808 (1956).
Lewis, T. B., Nielsen, L. E., *Trans. Soc. Rheol.* **12**, 421 (1968).
Lewis, T. B., Nielsen, L. E., *J. Appl. Polym. Sci.* **14**, 1449 (1970).
Nielsen, L. E., *Appl. Polym. Sympos.* **No. 12**, 249 (1969).
Nielsen, L. E., *J. Appl. Phys.* **41**, 4626 (1970).
Rosen, B. W., *Proc. Roy. Soc., Ser. A* **319**, 79 (1970).
Springer, G. S., Tsai, S. W., *J. Compos. Mater.* **1**, 166 (1967).
Sundstrom, D., Chen, S., *J. Compos. Mater.* **4**, 113 (1970).
Sundstrom, D., Lee, Y-D., *J. Appl. Polym. Sci.* **16**, 3159 (1972).
Tsai, S. W., U. S. Dept. of Commerce Rept. AD834-851 (1968).
Tsao, G. T., *Ind. Eng. Chem.* **53**, 395 (1961).
Whitney, J. M., Riley, M. B., *AIAA J.* **4**, 1537 (1966).
Zinsmeister, G. E., Purohit, K. S., *J. Compos. Mater.* **4**, 278 (1970).

Received for review September 29, 1972
Accepted July 30, 1973

Kinetics of a Moving Boundary Ion-Exchange Process

Paul R. Dana[1] and Thomas D. Wheelock*

Department of Chemical Engineering, Iowa State University, Ames, Iowa 50010

The acid elution of the dark blue cupric ammine complex from a cation-exchange resin produced a sharply defined moving boundary within each bead, which was photographed and measured to provide rate data. Analysis of the data by means of a theoretical model indicated that the overall elution process was controlled by a combination of internal and external mass transfer when acid concentrations less than 1.0 *N* were employed. At these acid concentrations the interdiffusion coefficient for the resin phase was found to be 3×10^{-6} cm^2/sec, independent of acid concentration but somewhat dependent on particle size. Data collected at higher acid concentrations were not amenable to analysis by the method employed. The model should be useful for predicting the time required to elute the cupric ammine complex or for designing equipment to carry out this process.

Introduction

The theoretical possibility of moving boundary processes in ion-exchange beads was suggested by Helfferich (1965). He anticipated that such processes would result when conversion of the resin involves consumption (or fixation) of the entering ion by a chemical reaction which is fast compared to diffusion. Generally such processes cannot be observed directly. However, while studying the ion-exchange behavior of the deep blue copper ammine complex, it was discovered that the acid elution of this complex from a strong-acid resin bead proceeds by a shrinking core process which can be followed readily because of a distinct color change. The color change is due to the destruction of the copper ammine complex by the hydrogen ions which penetrate the resin, thereby producing the following reaction within the resin phase

$$\overline{Cu(NH_3)_n^{2+}} + n\overline{H^+} \longrightarrow \overline{Cu^{2+}} + n\overline{NH_4^+} \tag{1}$$

(The overbars used in this and subsequent expressions designate the resin phase.)

The process described here differs from ordinary ion exchange where there is no accompanying chemical reaction except ion exchange and where all of the counterions in any given resin bead are thought to diffuse simultaneously so that no moving boundary develops. It has been found that the rates of ordinary ion-exchange processes are controlled either by film diffusion, intraparticle diffusion, or a combination of both (Boyd, *et al.*, 1947). Film diffusion tends to be the rate-controlling mechanism when high capacity resins of small diameter and low degree of cross-linking are contacted with slowly moving, dilute solutions, and conversely intraparticle diffusion tends to control when highly cross-linked, low-capacity resins are contacted with rapidly moving, concentrated solutions (Helfferich, 1962). Furthermore, the initial stage of an ion-ex-

[1] Present address, Dupont Co., Wilmington, Del.

change process is always controlled by film diffusion regardless of whether the later stage is controlled by film diffusion or intraparticle diffusion.

The purpose of the work described here was to investigate the kinetics of the overall process of acid elution of the cupric ammine complex from a widely used ion-exchange resin. For this purpose a photographic technique was developed and used to measure the movement of the sharp boundary which developed during the elution of a resin bead. The technique was subsequently applied to beads of different size which were eluted under various conditions of acid concentration and flow rate. A theoretical model of the process based on the assumption that the rate is controlled by a combination of film and intraparticle diffusion provided a means for analyzing the results.

Theoretical Model

For purposes of analysis it was assumed that individual ion-exchange beads were spherical and homogeneous and that they underwent negligible shrinking and swelling during the process of elution. It was also assumed that the overall rate of the process was controlled by a combination of film and intraparticle diffusion and that Fick's law with a constant effective diffusion coefficient was applicable to the resin phase. For any given component i this law is expressed as

$$J_i = -D \text{ grad } C_i \tag{2}$$

It was further assumed that mass transfer through the film was governed by the well known expression

$$J_i = k_m(C_0 - C_s) \tag{3}$$

with constant film coefficient.

More than two counterdiffusing species were involved in the present case (H^+, Cu^{2+}, NH_4^+) and due to the stoichiometry of the process, 1.22 moles of hydrogen ions diffused into the resin for each mole of cupric and ammonium ions which diffused out. Because the solutions were dilute, any convective effects resulting from unequal molar fluxes should have been negligible. Although the molar fluxes in opposite directions were unequal, the fluxes in terms of electrical equivalents were equal in order to maintain electroneutrality. In this regard the sulfate coions should have been excluded from the resin by the Donnan potential. In view of the presumed rigid coupling between fluxes, only the flux of the hydrogen ions was considered in the analysis which follows.

The diffusion process within an individual bead was represented by a material balance equation and certain initial and boundary conditions which were in keeping with the preceding assumptions. Thus, the material balance for the hydrogen ions within the reacted portion of a resin bead was represented by the following partial differential equation

$$D\left[\frac{\partial^2\bar{C}}{\partial r^2} + \frac{2}{r}\frac{\partial\bar{C}}{\partial r}\right] = \frac{\partial\bar{C}}{\partial t} \qquad (R > r > r_c) \tag{4}$$

The initial condition was taken to be

$$r_c = R \qquad (\text{at } t = 0) \tag{5}$$

The boundary condition used at the surface of the resin bead was

$$D\left(\frac{\partial\bar{C}}{\partial r}\right)_R = k_m\left(C_0 - \frac{\bar{C}_s}{\lambda}\right) \tag{6}$$

and the boundary conditions used at the moving interface between the reacted and unreacted portions of the bead were

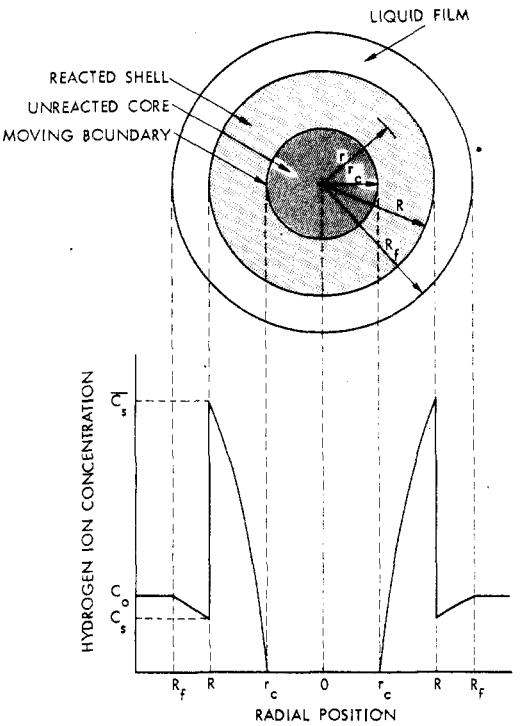

Figure 1. Theoretical concentration profile

$$(\bar{C})_{r_c} = 0 \tag{7}$$

$$D\left(\frac{\partial\bar{C}}{\partial r}\right)_{r_c} = -\bar{C}_r\left(\frac{dr_c}{dt}\right) \tag{8}$$

The meaning of these symbols is illustrated by Figure 1. In order to relate the concentration of the hydrogen ions inside the resin to the concentration outside, it was assumed that an equilibrium condition existed across the surface of the bead which could be represented by the expression

$$\lambda = \bar{C}_s/C_s \tag{9}$$

This relation is incorporated in eq 6. For any given run the distribution coefficient λ was assumed to be constant.

The preceding set of equations was solved by employing the quasi-steady-state approximation as Levenspiel (1962) and others have done. By means of this simplification eq 4 was reduced to

$$D\left[\frac{\partial^2\bar{C}}{\partial r^2} + \frac{2}{r}\frac{\partial\bar{C}}{\partial r}\right] = 0 \tag{10}$$

The solution of eq 10 together with the conditions imposed by eq 5 to 8 provided the following expression for the time required for the moving boundary to advance from R to r_c

$$t = \frac{R^2\bar{C}_r}{6C_0}\left[\frac{2(1-\xi^3)}{k_mR} + \frac{1-3\xi^2+2\xi^3}{\lambda D}\right] \tag{11}$$

where $\xi = r_c/R$. For convenience the group $k_mR/2$ was replaced by k which resulted in

$$t = \frac{R^2\bar{C}_r}{6C_0}\left[\frac{(1-\xi^3)}{k} + \frac{1-3\xi^2+2\xi^3}{\lambda D}\right] \tag{12}$$

The time required to complete the reaction of the bead corresponded to the value given by eq 12 when $\xi = 0$ or

$$T = (t)_{r_c=0} = \frac{R^2\bar{C}_r}{6C_0}\left[\frac{1}{k} + \frac{1}{\lambda D}\right] \tag{13}$$

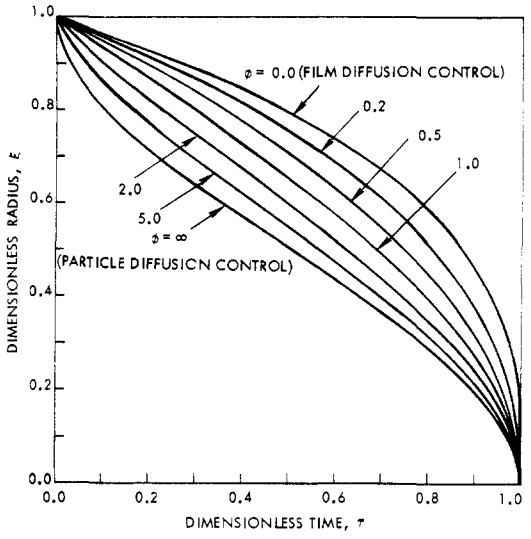

Figure 2. Position of the moving boundary as given by eq 14

Finally dividing eq 12 by eq 13 yielded the following expression in dimensionless form relating the position of the moving boundary to time of reaction

$$\tau = \frac{t}{T} = \frac{(1 - \xi^3) + \phi(1 - 3\xi^3 + 2\xi^3)}{1 + \phi} \tag{14}$$

where $\phi = k/\lambda D$.

Where the rate is controlled by intraparticle diffusion alone so that $k \gg \lambda D$, $C_0\lambda = \bar{C}_s$, and $\phi \rightarrow \infty$, eq 11 to 14 reduce to the expressions derived by Levenspiel (1962), Weisz and Goodwin (1963), and Helfferich (1965).

Figure 2 is a plot of eq 14 for different values of ϕ ranging from zero to infinity. The zero value of ϕ would correspond to the case where the rate of the process is controlled by film diffusion alone whereas the infinite value would correspond to the case where the rate is controlled by intraparticle diffusion alone. Of course, in between these limiting values the rate would be controlled by a combination of both film and intraparticle diffusion.

Interestingly enough for intermediate values of ϕ, the transient process described by the model would be controlled initially by film diffusion, most of the time by both film and intraparticle diffusion, and finally by intraparticle diffusion alone. This can be seen by inspection of the following relation between $\bar{C}_s$, the hydrogen ion concentration at the surface of the bead, and r_c, the radial position of the moving boundary

$$\bar{C}_s = k_m C_0 \left[\frac{D}{\left[\frac{1}{r_c} - \frac{1}{R}\right]R^2} + \frac{k_m}{\lambda} \right]^{-1} \tag{15}$$

For values of r_c approaching R this expression reduces to $\bar{C}_s = 0$ which corresponds to a film diffusion controlled process. On the other hand, for values of r_c approaching zero, this expression reduces to $\bar{C}_s = \lambda C_0$ which is equivalent to $C_s = C_0$ since $\bar{C}_s = \lambda C_s$ by definition. Of course, this eventuality corresponds to an intraparticle diffusion controlled process.

The theoretical model presented here predicts concentration profiles such as the one shown in Figure 1. Thus the concentration profile within the reacted shell of an individual bead is given by the expression

$$\frac{\bar{C}}{C_0} = \frac{k_m \lambda R^2 \left[\frac{1}{r_c} - \frac{1}{r}\right]}{k_m R^2 \left[\frac{1}{r_c} - \frac{1}{R}\right] + \lambda D} \tag{16}$$

Experimental Method

Resin Preparation and Analysis. The ion-exchange material employed in this investigation was a sulfonated copolymer of styrene and 8% divinylbenzene known as Dowex HCR-M resin which was a special designation for Dowex 50WX8 resin of 16-20 mesh size. The resin was preconditioned by backwashing it in a column with water to remove broken and very fine particles and then by contacting it with a series of aqueous reagents (sodium chloride, sulfuric acid, ammonium sulfate, and copper ammine sulfate). The concentration of each of the first three reagents was 2 N while the concentration of the copper ammine sulfate was 0.25 M. The copper solution also contained a large excess of ammonia. Between each successive contact and after the final contact with the copper-containing solution, the resin was washed thoroughly with distilled water. The preconditioned beads were dark blue in color, indicating the presence of the copper ammine complex.

A number of preconditioned Dowex HCR-M beads were analyzed individually for their copper content. The diameter of each bead was measured first and then the bead was placed in a test tube and eluted with a large excess of sulfuric acid. Subsequently, the copper content of the resulting solution was determined with an atomic absorption spectrophotometer. The results of this analysis which are presented in Figure 3 indicate a relationship between the copper content or loading of the beads and their diameter. The straight line plotted in Figure 3 represents the linear regression

$$M = 0.1491 - 0.539R \tag{17}$$

The numerical coefficients were found by the method of least squares. The average loading of all the beads was 0.1226 g of Cu/cm^3 of resin, which corresponds to 3.86 equiv/l. This value should have been close to the average concentration of fixed ionic groups in the resin.

Several bulk samples of preconditioned Dowex HCR-M resin were analyzed for both copper and ammonia contents. Each sample was placed in a column and eluted with excess sulfuric acid. The concentration of ammonia in the column effluent was determined by the Kjeldahl method. Copper was extracted from the Kjeldahl residue and determined with an atomic absorption spectrophotometer. According to this analysis, the average ratio of ammonia to copper in the preconditioned resin was 3.48. Consequently, 3.48 moles of hydrogen ions were required to break 1.0 mole of the cupric ammine complex in accordance with eq 1 or a total of 5.48 moles of hydrogen ions were needed for the complete elution of 1.0 mole of the complex. Combining this result with eq 17 provided the means shown below for expressing the concentration of the preconditioned resin in terms of the equivalents of hydrogen ions required to elute the resin.

$$\bar{C}_r = 12.86 - 46.5R \tag{18}$$

Rate Measurement. The cell shown in Figure 4 was used in determining the rate of advance of the sharp moving boundary which developed during the acid elution of resin beads containing the copper ammine complex. This cell was constructed from the body of a number 3, oblique bore, ground-glass stopcock. The resin beads were supported in the cell by a fine-mesh Saran screen which was held between Plexiglas washers attached to the stopcock body with epoxy cement.

For a typical run sulfuric acid of known concentration was conducted through the cell at a controlled rate and the acid level in the cell was maintained about 1 cm above the screen support. After the acid flow was estab-

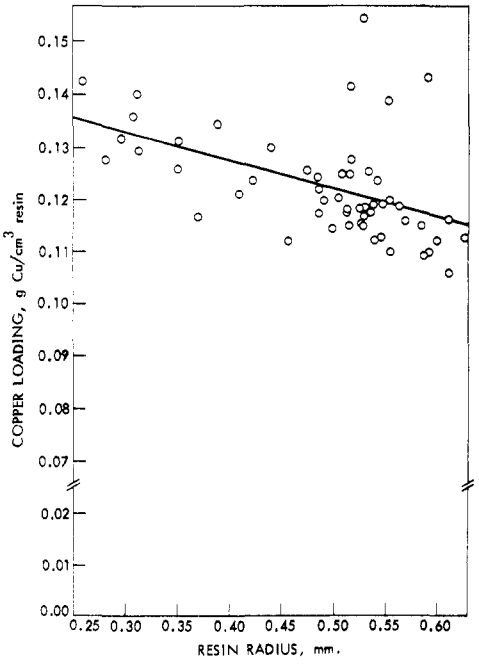

Figure 3. The copper content or loading of individual Dowex HCR-M resin beads

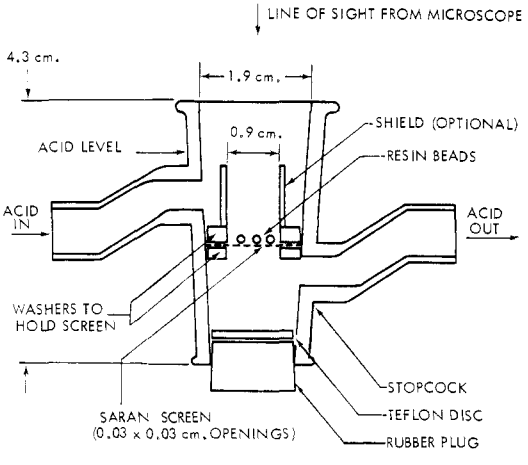

Figure 4. Cell used for eluting the resin beads

lished, about a dozen carefully selected, preconditioned resin beads were placed on the screen and these were observed and photographed with a Bausch and Lomb Model BVB-73 stereo zoom microscope which was fitted with a stereo camera attachment employing 35-mm Ektachrome Type B film. During a typical run pictures were taken at 10–30-sec intervals using a magnification of 15–20× and an exposure time of 0.5 sec. The exact time when each picture was taken was registered by a strip chart recorder connected to the camera shutter. The beads were illuminated from above with a high-intensity lamp. Any given run was discontinued after all of the beads were completely eluted as indicated by the disappearance of the blue core. The photographs of beads taken at various stages of elution were projected on a screen and the diameter of each bead and its blue core was measured. A scale of measurement for each set of photographs was provided by photographing a stage micrometer viewed through the microscope using the same magnification as was employed in photographing the beads. A correction was applied to the core measurements to account for the refraction of light at the fluid–particle interface.

Results

A series of experimental runs were made at room temperature (77°F) and pressure using the technique described above to measure boundary movement. In this series bead diameter was varied between 0.050 and 0.13 cm, acid concentration between 0.05 and 5.06 N, and acid flow rate between 0 and 2.0 ml/sec.

Typical results are presented in Figure 5, which shows the set of resin beads in run 297 at various stages of elution. These photomicrographs were made at the indicated time measured from the instant when the beads were placed in the cell. From these and many other similar pictures it was possible to see that the dark blue spherical core receded uniformly within each bead until it reached the mathematical center where it disappeared. Occasionally the dark core would be distorted as in the case of the larger bead in the lower left-hand corner (Figure 5) because of a crack or other defect. Moreover, the cores of beads which were touching each other or touching the wall of the cell did not recede uniformly. In all cases where the core receded uniformly, the moving boundary remained sharp until the core reached the center point and disappeared. Although the position of the boundary could not be determined accurately in the beginning, by the time the core had reached a diameter which was 86% of the bead diameter, its position was clearly established. In the photomicrographs it can be seen that it generally required more time to elute the larger beads than the smaller ones. Moreover, beads of the same size did not always elute at the same rate. This difference in rates may have been due to lack of uniformity in the flow field or to differences in the beads themselves. During the elution process the overall diameter of individual beads changed very little so there was justification for neglecting shrinking and/or swelling effects.

A preliminary analysis of the data was made by plotting the position of the moving boundary as a function of time for individual beads using the dimensionless coordinates of Figure 2. The resulting plots were then compared with Figure 2, and this showed that for acid concentrations of 1.0 N and less, the proposed model might well represent the elution process but for higher acid concentrations it could not since the data always fell below the family of curves shown in Figure 2. It is noteworthy that Selim and Seagrave (1973) found that with higher acid concentrations this process could be represented by a model which only accounted for intraparticle diffusion provided the quasi-steady-state approximation was not made.

For the lower acid concentrations where our model seemed to apply, nonlinear regression analysis was used subsequently to determine the best values of k and λD in eq 12 for individual beads. This computation was made with a digital computer using a general program described by Atkinson (1966) for fitting nonlinear regression functions by least squares based on a modified Gauss Newton method. For representative beads estimated values of k and λD were then used with eq 12 to predict the position of the moving boundary as a function of time. Figure 6 is typical of the results obtained. The fit between the predicted curve and the experimental points was generally quite good. The major discrepancy was at the beginning where the first few points could not be determined accurately. Hence, these points were omitted in calculating k and λD. The generally close fit between the calculated curve and measured points provided strong support for the proposed model.

Values of k and λD determined by nonlinear regression analysis were averaged over the beads in each run and the ratio of the average values of these parameters was ob-

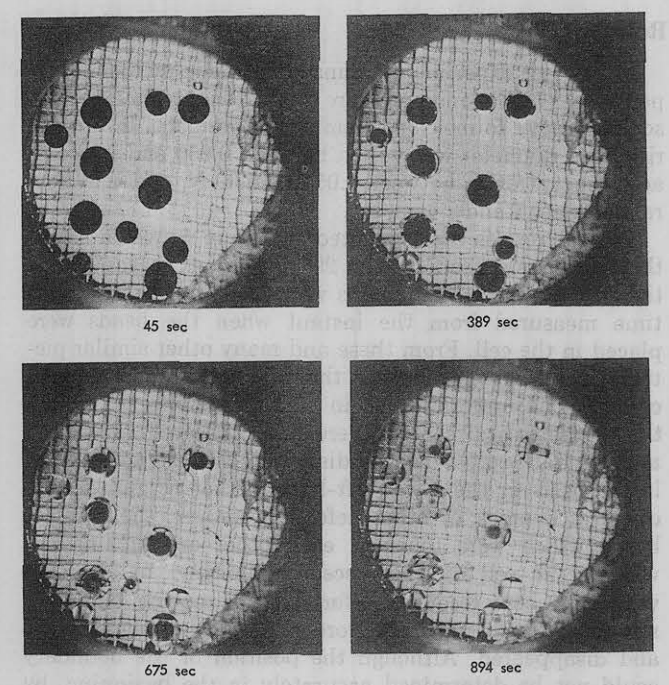

Figure 5. Resin beads at various stages of elution in run 297

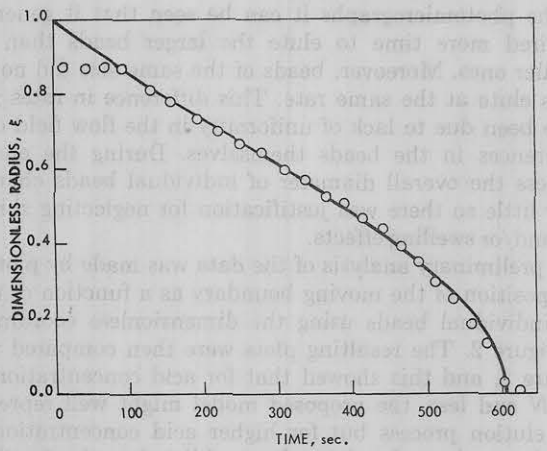

Figure 6. Moving boundary data from run 279, bead no. 10, and the smooth curve predicted by theory

tained to estimate ϕ for each run (Table I). In general the value of k was several times larger than that of λD, indicating the relative greater importance of intraparticle diffusion in controlling the overall rate. It was only where either the acid concentration or flow rate was very small that k was smaller than λD. Since the ratio of k to λD increased as acid concentration increased, it is apparent that film diffusion became less important as the acid concentration increased.

The standard deviations of both k and λD from their respective means were also calculated for each run (Table I). In all instances where k was larger than λD, the standard deviation of k was larger than the standard deviation of λD and where k was smaller its standard deviation was also smaller. Thus the variation in k was greatest where the method of evaluating k was probably the least sensitive to k and the variation least where the method was most sensitive. The same thing also appeared true with regard to the variation in λD. Some of the variation in both k and λD was due to the use of eq 18 to predict $\overline{C}_r$ since individual beads varied from this relationship. In addition some of the variation was due to either the direct or indirect effects of particle size since beads of different

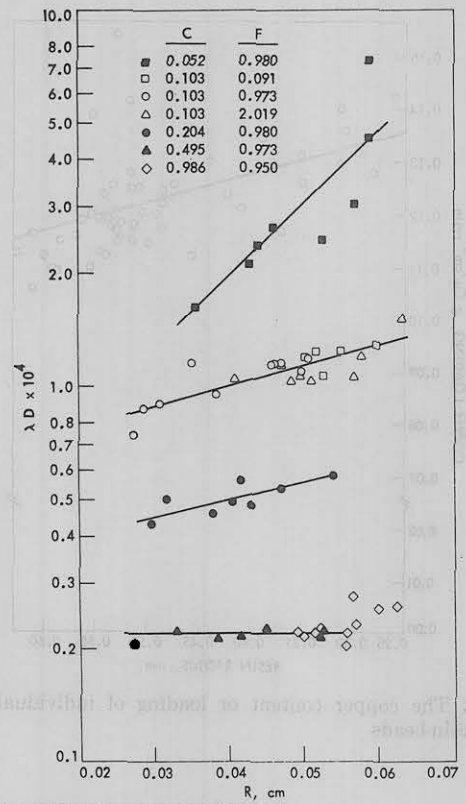

Figure 7. Values of λD for individual beads

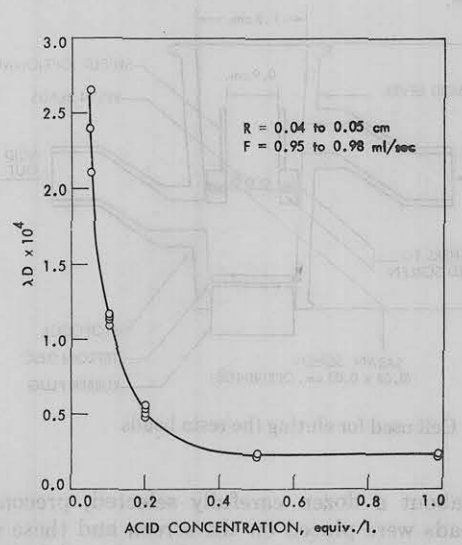

Figure 8. Values of λD for individual beads of similar size

size were used in each run. For a stagnant fluid, k (but not k_m) should have been independent of particle size but for a moving fluid it should have been somewhat dependent on particle size (Sherwood and Pigford, 1952). When the effect of film diffusion was significant, λ would not have been constant during a given run as assumed and the change in λ could have been responsible for some of the variation in both k and λD which appeared due to particle size. Additional variation in k may have resulted from distortion of the flow field because the apparatus was not designed to provide a uniform field.

Values of λD for individual beads are plotted in Figure 7 to illustrate the possible effects of particle size, acid concentration, and flow rate on this parameter. It can be seen that λD was greatly affected by concentration which is not surprising since the equilibrium distribution coefficient λ is known to be dependent on concentration. Fur-

Table I. Average Values of Parameters in Eq 12 and 14

Run no.	Acid normality	Flow rate, ml/sec	$k \times 10^6$ cm²/sec	$S_k \times 10^6$ cm²/sec	$\lambda D \times 10^6$ cm²/sec	$S_D \times 10^6$ cm²/sec	ϕ
193	0.986	0.95	163.9	60.2	23.4	2.4	7.0
272	0.495	0.97	150.6	73.8	21.7	0.8	6.9
279	0.103	0.97	265.7	191.5	103.6	15.7	2.6
284	0.103	0.09	99.7	8.1	120.6	83.8	0.8
287	0.103	2.02	316.5	91.7	113.9	16.7	2.8
295	0.204	0.98	141.9	26.3	51.2	5.0	2.8
297	0.052	0.98	170.5	33.8	327.1	185.8	0.5

Table II. Average Diffusion Coefficients

Run no.	Acid normality	λ	$D \times 10^6$ cm²/sec	$D \times 10^6$ cm²/sec[a]
193	0.986	3.91	5.98	5.63
272	0.495	7.80	2.78	2.84
279	0.103	37.5	2.76	3.03
284	0.103	37.5	3.21	3.17
287	0.103	37.5	3.03	2.86
295	0.204	19.0	2.70	2.74
297	0.052	74.1	4.42	3.22

[a] D based on beads of size $R = 0.04$ to 0.05 cm.

thermore, it can be seen that λD was not affected noticeably by flow rate and it should not have been. Finally, it can be seen that λD was affected by particle size at the lower acid concentrations and this was probably due to the error in assuming λ to be constant for any given run (Helfferich, 1972). Figure 7 also shows the scatter in λD. The variation was greatest at the lowest acid concentration where the sensitivity to λD was probably least.

To further illustrate the effect of acid concentration on λD, Figure 8 is presented. Only data for beads having a radius between 0.04 and 0.05 cm are included so as to minimize the variation due to particle size.

In order to estimate λ it was assumed that in the process described here the cupric and ammonium ions were washed away as they diffused out of the beads so the concentrations of these ions on either side of the liquid-bead interface should have been much smaller than the corresponding concentrations of hydrogen ions. Furthermore, it was assumed that there was no invasion of electrolyte over that of the fixed ionic groups in the resin. As a consequence of these assumptions, the concentration of hydrogen ions inside the resin phase near the bead surface should have been nearly equal to the concentration of fixed ionic groups, 3.86 equiv/l., and λ could be evaluated by employing the relation

$$\lambda = 3.86/C_0 \tag{19}$$

Admittedly the first of these assumptions would be valid where the effect of film diffusion is negligible (high acid concentrations) whereas the second would be valid at low acid concentrations. Hence, eq 19 was only approximate at best, but since experimental equilibrium data were lacking, it was used to estimate the values of λ presented in Table II.

The average values of λD listed in Table I were subsequently divided by the estimated values of λ to obtain the average diffusion coefficients shown in Table II. In addition, the average diffusion coefficients of beads limited to the size range of $R = 0.04$ to 0.05 cm were found by a similar process. It can be seen that the two sets of values are nearly the same with the greatest difference being in the values for run 297 which exhibited the greatest effect due to bead size (Figure 7). More importantly, the value of the diffusion coefficient was nearly constant, being approximately 3×10^{-6} cm²/sec over the concentration range from 0.05 to 0.5 equiv/l. Although this value is similar in magnitude to the value of 5.4×10^{-6} cm²/sec reported by Inczédy (1966) for diffusion of hydrogen ions in Dowex 50X8 resin, it must be taken into consideration that the present process involved the counterdiffusion of different ionic species. The constancy of the diffusion coefficient added further support to the applicability of the proposed model.

Conclusions

The acid elution of the cupric ammine complex from Dowex HCR-M ion-exchange resin provides a good example of a moving boundary process which can be observed closely because of a distinct color change. With acid concentrations between 0.05 and 1.0 N, the rate of the overall process appears to be controlled by a combination of film and intraparticle diffusion. At the lower end of the concentration range, film diffusion seems to predominate; at the upper end, intraparticle diffusion predominates. The effective diffusion coefficient for the resin phase is approximately 3×10^{-6} cm²/sec, independent of acid concentration, but somewhat dependent on particle size. The particle size dependency is believed due in part to the incorporation of a constant phase distribution coefficient in the model used for analyzing the data.

Acknowledgment

The careful critique and helpful suggestions of Dr. F. G. Helfferich are acknowledged gratefully.

Nomenclature

C = hydrogen ion concentration of the external phase, M
$\bar{C}_r$ = concentration of uneluted resin expressed in terms of hydrogen ions required for elution, M
D = effective interdiffusion coefficient, cm²/sec
F = solution flow rate, ml/sec
J = mass flow, mequiv/(sec)(cm²)
k = mass transfer coefficient group, $k_m R/2$, cm²/sec
k_m = film mass transfer coefficient, cm/sec
M = copper loading of resin, g/cm³
n = ratio of ammonia to copper in the cupric ammine complex, dimensionless
r = radial position in bead, cm
R = bead radius, cm
S_D = standard deviation of D, cm²/sec
S_k = standard deviation of k, cm²/sec
T = time required to completely elute an individual bead, sec
t = bead elution time, sec

Greek Letters

λ = molar distribution coefficient for hydrogen ions, dimensionless
ξ = radial position of moving boundary, dimensionless
τ = bead elution time, dimensionless
ϕ = dimensionless group, $k/\lambda D$

Literature Cited

Atkinson, J. D., "TARSIER," Numerical Analysis Programming Series No. 8, Statistical Laboratory, Iowa State University, Ames, Iowa, 1966.
Boyd, G. E., Adamson, A. W., Myers, L. S., Jr., *J. Amer. Chem. Soc.* **69**, 2836 (1947).

Helfferich, F. G., "Ion Exchange," Chapter 6, McGraw-Hill, New York, N. Y., 1962.
Helfferich, F. G., *J. Phys. Chem.* **69**, 1178 (1965).
Helfferich, F. G., Shell Development Co., Houston, Tex., private communication, 1972.
Inczédy, J., "Analytical Applications of Ion Exchangers," English translation by A. Páll, p 68, Pergamon Press, New York, N. Y., 1966.
Levenspiel, O., "Chemical Reaction Engineering," p 346, Wiley, New York, N. Y., 1962.
Selim, M. S., Seagrave, R. C., *Ind. Eng. Chem., Fundam.* **12**, 14 (1973).
Sherwood, T. K., Pigford, R. L., "Absorption and Extraction," pp 72–74, McGraw-Hill, New York, N. Y., 1952.
Weisz, P. B., Goodwin, R. D., *J. Catal.* **2**, 397 (1963).

Received for review October 11, 1972
Accepted September 10, 1973

This work was supported by the Engineering Research Institute, Iowa State University, Ames, Iowa.

Surface Shear Viscosity and Related Properties of Adsorbed Surfactant Films

Lalit Gupta and Darsh T. Wasan*

Department of Chemical Engineering, Illinois Institute of Technology, Chicago, Ill. 60616

The adsorption and accumulation of surface-active agents at fluid–fluid interfaces results in additional, intrinsic, hydrodynamic resistance to flow of which surface shear viscosity is a measure. The results of a study of the surface shear viscosity of a number of soluble surfactant systems are presented. None of the nonbiodegradable, single-component soluble surfactants investigated yielded significant surface shear viscosities. However, lauric acid and lauryl alcohol, practically insoluble in water by themselves but solubilized by sodium lauryl sulfate, yielded significant surface shear viscosities at certain concentrations and proportions. Relatively insoluble substances or such substances solubilized by other substances will usually cause significant surface shear viscosity at liquid–gas interfaces.

Introduction

An understanding of many engineering operations such as distillation, gas absorption and desorption, and liquid–liquid extraction is contingent on a thorough study of the role of the interfaces across which transport occurs. In this context, interfacial properties and the dynamic effects of surfactants thereon assume importance. The significance of interfacial shear viscosity has been recognized in several instances such as foam fractionation, formation and stability (Kanner and Glass, 1969; Leonard and Lemlich, 1965; Mannheimer, 1969; Miles, *et al.*, 1950; Shah, 1972; Shih and Lemlich, 1967; Whitaker, 1966), emulsion stability (Oldroyd, 1955; Sherman, 1953), suspension polymerization (Joly, 1964; Kanner and Glass, 1969), film permeability (Cadenhead, 1969; Joly, 1964, 1972a,b), tanning (Joly, 1964), Marangoni instability (Scriven and Sternling, 1964; Sternling and Scriven, 1959), lung surfactant systems (Scarpelli, 1968), films flowing down solid walls (Whitaker, 1964; Whitaker and Jones, 1966), bubble and drop behavior (Bupara, 1966), and mass transfer operations (Lewis, 1954a,b).

Surface-active agents tend to accumulate and adsorb at the interfaces between their solutions and the adjacent solid, liquid, or gaseous phases. Such accumulation at fluid–fluid interfaces results in additional, intrinsic, hydrodynamic resistance to flow. Interfacial shear viscosity is a measure of this resistance. It is defined as the ratio of the interfacial shear stress to the interfacial shear rate and has the dimensions (M/T), or in the cgs system g/sec or surface poise (s.p.).

The concept of interfacial shear viscosity originated more than a hundred years ago (Plateau, 1869). Since then, interfacial shear viscosity and its measurements have received considerable attention (Joly, 1964; Pintar, 1968). The earlier observations of interfacial shear viscosity were made at liquid–gas interfaces and were mainly concerned with insoluble monomolecular films. These studies are reviewed by Gaines (1966), Kanner (1968), and Joly (1956, 1964, 1972a,b). It is only in recent years that attempts have been made to extend interfacial shear viscosity measurements to liquid–liquid interfaces (Gupta, 1970; Wasan, 1971; Wasan, *et al.*, 1971) and to films at liquid–gas interfaces adsorbed from surfactant systems (Eirich, 1967; Joly, 1964).

A survey of the literature on the surface shear viscosity of soluble surfactant films at liquid–gas interfaces revealed only isolated pieces of work (Brown, *et al.*, 1953; Israel, 1968; Joly, 1964; Karam, *et al.*, 1967; Lorinc, 1969; Mannheimer, 1969; Mannheimer and Schechter, 1970; Ross and Epstein, 1958; Trapeznikov and Dokukina, 1970; Vocel and Ryan, 1971; Vora, 1970) in the field. Often, the reported values are close to the sensitivity of the measurement technique. In certain cases the surfactants used were not 100% active or underwent degradation. Also, in most cases, the lack of a mathematical analysis permitting an exact relationship between surface viscosity and experimentally measured variables does not justify full confidence in the reported values of surface viscosity. An experimental program was therefore undertaken to gain insight into the kind of surfactants that would yield significant surface viscosities. Having identified such systems, measurements would then be made of other properties like surface tension, surface potential, and light scattering ratios to shed light on the characteristics of interfacial films.

Theoretical Considerations

Surface Shear Viscosity. Surface shear viscosity was determined by the so-called deep-channel viscous traction interfacial viscometric technique (Burton and Mannheim-